Arch. Biol. Sci., Belgrade, 67 (1), 69-81, 2015 DOI:10.2298/ABS140124002M

LYMPHOCYTES' 'LAST STAND' ON THE NUCLEAR MATRIX AFTER WHOLE BODY EXPOSURE OF RATS TO LOW-LET IONIZING RADIATION

Vesna I. Martinović[1,*], Žarko Ivanović[2], Mirjana Mihailović[1], Svetlana K. Ivanović-Matić[1], Goran Đ. Poznanović[1] and Melita S. Vidaković[1]

[1] *Department of Molecular Biology, Institute for Biological Research "Siniša Stanković", University of Belgrade,* Bulevar Despota Stefana 142, 11060 Belgrade, Serbia
[2] *Department of Plant Disease, Institute for Plant Protection and Environment,* Teodora Drajzera 9, 11000 Belgrade, Serbia

[*]Corresponding author: vecam@ibiss.bg.ac.rs

Abstract – We examined the functions of the rat lymphocyte nuclear matrix after a single exposure to total body irradiation with doses ranging from sublethal to lethal. Irradiation induced systemic oxidative stress, detected as increased activities of serum SOD and catalase, lymphocyte DNA damage, detected by the Comet assay, and apoptosis. After irradiation with lower doses, the recruitment of DNA repair centers on the matrix was observed by Western analysis as increased levels of matrix-associated PARP-1, p53 and PCNA. Augmented partitioning of the pro-survival transcription factor NF-κB on the matrix was also detected after irradiation. Exposure to a lethal dose caused breakdown of the matrix, observed as lamin B cleavage, and of the matrix-associated DNA repair centers, detected as caspase-mediated PARP-1 proteolysis and loss of protein associations with the matrix. These findings suggest that the nuclear matrix establishes functional interactions in a defensive mechanism, integrated in a decision-making process that resolves cell fate.

Key words: DNA repair; ionizing radiation; NF-κB; nuclear matrix; p53; PARP-1; PCNA

Abbreviations: NF-κB – nuclear factor kappa-light-chain-enhancer of activated B cells; p53 – tumor suppressor phosphoprotein 53; PARP-1 – poly(ADP-ribose) polymerase-1; PCNA – proliferating cell nuclear antigen; ROS – reactive oxygen species; SOD – superoxide dismutase

Received January 24, 2014; **Accepted** March 2, 2014

INTRODUCTION

The ionizing property of radiation possesses a high potential to damage living organisms. Types of radiation differ in their constituent ionizing particles (electrons, protons, neutrons, etc.) and their energy. Radiation that causes dense ionization along its track is referred to as high-linear-energy-transfer (high-LET) radiation according to the physical parameter used to describe the average energy released per unit length of their pathway or track. Low-LET radiations produce ionizations sparingly along their track and therefore almost homogeneously within a cell. Thus, high-LET radiations are more destructive to biological material than low-LET radiations, whereas high-LET radiations, such as neutrons and

α particles, transfer most of their energy to a small region of the cell (Dendy and Brugmans, 2003; Feinendegen, 2003; Feinendegen, 2005). Aside from the direct and immediate damage that low-LET X-rays cause to biological molecules, reactive oxygen species (ROS) that are subsequently formed from water and molecular oxygen lead to further damage. Thus, fewer DNA strand breaks are observed immediately after irradiation than after 30-60 min when the maximum number of breaks occurs (Holt et al., 2009). High doses of radiation induce oxidative stress with a pronounced decrease in antioxidant capacity (Chevion and Berry, 1999) which leads to different types of damage at the molecular and cellular levels, (Farber 1994; Loft and Poulsen 1996; Klauning et al. 1998), and when ROS levels exceed the cellular antioxidant capacity, cells begin to die (Oberly and Oberly 1986).

Various forms of damage can be generated on DNA, including base damage, base loss, single- and double-strand breaks or any combination thereof. The cell repair systems manage to completely restore the DNA sequence without alterations of ongoing cellular processes in most simple lesions. However, in the case of more complex lesions, DNA repair is synchronized with cellular processes such as cell cycle regulation and differentiation, and if the repair is not successful, the process of cell death is induced (Mori and Desaintes 2004) which eliminates mutated cells, reducing genomic instability in tissues (Feinedegen, 2005).

The nuclear matrix, a non-chromatin protein framework of the nucleus, has been implicated in many nuclear processes (Linnemann et al., 2009). Nuclear matrix dynamism is generally manifested by a variety of specific protein-protein (Dinić, et al., 2000; Ivanović-Matić et al., 2000; Grdović et al., 2003; 2005; Vidaković et al., 2004) and protein-DNA interactions (Poznanović et al., 1994; 1996; 1999; Bogojević et al., 2003). Therefore, it was assumed that some of these interactions could also be responsible for regulating the DNA repair process (Fackelmayer, 2004; Vidaković et al., 2005). One of the earliest nuclear events that follows DNA repair after DNA strand breakage caused by agents such as ionizing irradiation, alkylating agents or carcinogens, is the poly(ADP-ribosyl)ation of various proteins localized near the strand breaks. Poly(ADP-ribose) polymerase-1 (PARP-1) catalyzes the poly (ADP-ribosyl)ation of various nuclear proteins by binding to single- or double-stranded DNA ends. The targets for post-translational modification by PARP-1 are transcription factors that activate or suppress transcription of genes specific to the cells' response to the damaging agent or irradiation (Veuger et al., 2009). These proteins establish and maintain cellular functions necessary for damage recovery but can also direct the cell along the death pathway. An ionizing radiation signal initiates two chains of events. One is connected to the DNA repair system in which PARP-1 is recruited and activated by the presence of strand breaks, followed by the recruitment DNA repair "helper" proteins. Another chain of events engages proteins that are involved in cell signaling and is connected with cell cycle control and cell death, with the two post-irradiation events being closely interconnected (Vidaković et al., 2005).

Ionizing radiation induces significant morphological changes in lymphocytes that are rapidly cleared from the circulation. These are accompanied by single-strand and to a lesser extent double-strand breaks in the DNA. Circulating lymphocytes are highly radiosensitive and are sometimes referred to as biological dosimeters. Thus, they represent a useful model for examining some of the immediate effects of radiation exposure on living cells (Borehamd et al. 1996). We investigated whether the nuclear matrix provides a dynamic macromolecular platform that participates in the cell's defensive response by localizing the major DNA repair proteins, PARP-1, tumor suppressor protein p53 and proliferating cell nuclear antigen (PCNA), as well as the redox-sensitive, pro-survival transcription factor NF-κB during the early, rapid response to irradiation in the lymphocyte. In view of the significant energy expenditure by DNA repair, this defensive mechanism is integrated in a decision-making process that ultimately determines cell fate. Thus, the aim of this work was to assess whether the nuclear matrix provides the struc-

tural and functional backdrop for the cell's last line of defense.

MATERIALS AND METHODS

Animals and irradiation treatment

All animal procedures were in compliance with the EEC Directive (86/609/EEC) on the protection of animals used for experimental and other scientific purposes, and were approved by the Ethical Committee for the Use of Laboratory Animals of the Institute for Biological Research Siniša Stanković, University of Belgrade registered in the Serbian Laboratory Animal Science Association (SLASA) which is a member of the Federation of European Laboratory Animal Science Association (FELASA). Ten week old Wistar adult male rats weighing 220 g were maintained at 22°±1°C, 50%±5% humidity at 12 h light/dark intervals, and were provided with rat chow and drinking water *ad libitum*. The animals were randomized, placed in ventilated Plexiglas® container divided into 10 chambers. The container was covered with a 1 cm-thick Plexiglas® sheet. The animals were exposed to radiation at 100 cm distance from the source. Individual rats were irradiated either with a single sublethal (2.7 Gy; LD20), a mean lethal (5.4 Gy; LD50) or an absolutely lethal dose (10.8 Gy; LD100) of low-LET X-ray irradiation at a rate of 3.4 Gy/min, using a Philips linear accelerator SL 75-80, 8 MeV. One hour after irradiation the animals were killed, the peripheral blood was taken, treated with heparin and mixed with 1 x sterile phosphate-buffered saline (PBS; 4.3 mM Na_2HPO_4, 2.7 mM KCl, 1.8 mM KH_2PO_4, 137 mM NaCl, pH 7.4).

Isolation of lymphocytes

Peripheral blood mononuclear cells, lymphocytes and monocytes were isolated according to the protocol at: http://www.biolabprotocols.com/view/310/Human-Peripheral-Blood-Mononuclear-Cell-Preparation.html. Platelets, red blood cells and neutrophils are largely depleted from the final cell sample. Peripheral blood treated with anticoagulant was mixed at a ratio of 1.5:1 with sterile PBS (pH 7.4), followed by the addition of 1.5 ml of 0.6% dextran T 500 (Pharmacia) in PBS. Blood samples were mixed by inverting the tube four to five times. The mixture was kept undisturbed at room temperature for 20 min to allow the erythrocytes to sediment. The supernatant was transferred to a fresh tube and an equal volume of PBS containing 5 mM EDTA was added. The samples were centrifuged at 1 000 x g for 10 min at room temperature and the leukocytes were pelleted while the platelets were retained in the supernatant. The cell pellet was resuspended in PBS and gently layered onto Ficoll-Hypaque 1077 (SIGMA-ALDRICH). The suspension was centrifuged at 800 x g for 20 min at 12°C (with the brake turned off). The supernatant was removed and the lymphocytes that appeared as a cloudy ring at the PBS/Ficoll interface were collected. The harvested lymphocytes were washed twice in PBS and centrifuged at 800 x g for 10 min. The lymphocyte pellet was kept at -80°C in appropriate buffer supplemented with dimethyl sulfoxide (DMSO).

Isolation of lymphocyte nuclei and nuclear matrix proteins

Lymphocyte nuclei and nuclear matrices were prepared according to the modified procedure of Belgrader et al. (1991). The cells were washed two times with ice-cold PBS. The cell pellet was warmed to room temperature for 45 s, resuspended in TM-2 buffer (10 mM Tris-HCl, pH 7.4, 2 mM $MgCl_2$, 0.5 mM phenylmethylsulfonyl fluoride (PMSF) at 10°C to a density of 10^7 cells/ml, and incubated at room temperature for 1 min and then on ice for 5 min. Triton X-100 was added to 0.5% (v/v), and the cells were incubated on ice for 5 min. The cells were sheared by three passes through a 22 gauge needle. Nuclei were separated from the cytoplasm by centrifugation at 800 x g for 6 min at 4°C, washed twice in TM-2 buffer and temperature-stabilized at 42°C for 20 min in the same buffer. The nuclei were incubated 1 h on ice in TM-2 buffer supplemented with 2 mM sodium tetrathionate. $MgCl_2$ was added to the nuclei in TM-2 buffer to 5 mM final concentration. The nuclei were digested with 100 mg/ml DNase I in TM-0.2 (10 mM Tris-HCl, pH 7.4, 0.2 mM $MgCl_2$, 1 mM PMSF) for 1 h on ice. The bulk of the DNA and chromatin

proteins were extracted with 0.25 M $(NH_4)_2SO_4$ in TM-0.2 buffer by incubation on ice for 15 min and centrifugation at 5 000 x g for 15 min. The obtained nuclear matrices were stored resuspended in 0.25 M sucrose, 10 mM NaCl, 3 mM $MgCl_2$, 10 mM Tris-HCl, pH 7.4, 0.5 mM PMSF, and an equal volume of sterile glycerol at -20°C.

Comet assay

The comet assay was performed as described by Singh et al. (1994). A suspension of isolated lymphocytes and 0.5% low-melting agarose was overlayed onto precoated slides. The slides were immersed in cold lysis buffer at pH 10 (2.5 M NaCl, 100 mM EDTA, 10 mM Tris) and incubated at 4°C for 2 h. Following lysis, the slides were placed in alkaline electrophoresis buffer at pH 13 (300 mM NaOH, 1 mM EDTA) for 30 min to allow denaturation of the DNA. The slides were transferred to an electrophoresis tank with fresh alkaline electrophoresis buffer and separated at 1.33 V/cm, 0.01 kV-139 mA for 20-30 min (4°C). After neutralization in 0.4 M Tris-HCl, pH 7.4, for 15 min, the slides were stained with 100 µl SYBR® Green (SIGMA-ALDRICH) and examined under a fluorescent microscope (Leica DM LB, filter fluorescent emission at 520 nm). All the steps were conducted under yellow light or in the dark to prevent nonspecific DNA damage. At least one hundred cells per sample were analyzed and DNA damage was quantified. The comet assay essentially reflects the displacement of fluorescence from the head to the tail in damaged cells. The tail moment, incorporates the size of the smallest detectable migrating DNA, observed as the length of the comet, and the number of relaxed/broken DNA fragments observed as the intensity of total DNA in the tail. The tail moment was expressed as the percentage of the DNA in the tail, multiplied by the length between the center of the head and tail (Olive et al., 1990a).

DNA isolation and agarose gel electrophoresis

Lymphocytes were diluted in Modified Bradley Buffer (5 mM EDTA, 10 mM Tris-HCl, pH 8.0, 150 mM NaCl, 0.5 % SDS). Proteinase K was added to a final concentration of 100 µg/ml, the tubes were mixed and incubated overnight at 50°C. Total DNA was extracted with phenol-chloroform-isoamyl alcohol. DNA electrophoresis was performed in 1.5% agarose gels in 0.5 x Tris-borate/EDTA buffer.

Activity gel assays for superoxide dismutase and catalase

Blood was collected in tubes containing 1 000 IU heparin, and the plasma was separated by centrifugation at 3 000 x g for 10 min. The plasma was immediately immersed in liquid nitrogen and stored at -80°C. A total of 200 µg proteins/lane were separated in a native polyacrylamide gel (Laemmli, 1970); 12% and 8% gels were used for the SOD and catalase activity assays, respectively. SOD activity was determined according to Oberly and Spitz (1984). Catalase activity was determined according to Sun et al. (1988). The bands were quantified with a computerized imaging system using TotalLab (Phoretix) electrophoresis software (v 1.10).

PARP-1 activity assay

The PARP-1 activity assay is a universal colorimetric assay for screening and quantifying PARP-1 activity in cells (4677-096-KHT Universal Color PARP Assay Kit, Trevigen) was performed on isolated lymphocyte whole cell extracts according to the manufacturer's instructions.

SDS-PAGE and Western immunoblot analysis

Protein concentrations were determined according to Lowry et al. (1951). For sodium dodecyl sulfate-polyacrylamide gel electrophoresis (SDS-PAGE) 20 µg of proteins were loaded onto 4% stacking/12% separating slab gels as described by Laemmli (1970). Nucleoproteins separated by SDS-PAGE were transferred to PVDF membranes (Hybond-P, Amersham Pharmacia Biotech and Western immunoblot analysis was performed by Towbin et al. (1979). Immunoblot analysis was performed using rabbit polyclonal antibodies for caspase-3 (H-277), PARP-1 (H-250), NF-κB (p65; C-20), p53 (FL-393), PCNA (FL-261),

SOD2 (MnSOD) (FL-222), β-actin (C-11)-R, and goat polyclonal antibodies for SOD1 (CuZnSOD) (C-17), A/C lamins (N-18) and lamin B (M-20) (all from Santa Cruz Biotechnology). The blots were probed with horseradish peroxidase-conjugated goat anti-rabbit IgG, bovine anti-goat IgG (all from Santa Cruz Biotechnology). Staining was performed by the chemiluminescent technique according to the manufacturer's instructions (Santa Cruz Biotechnology).

Isolation of lymphocyte whole cell lysate

Lymphocytes were incubated on ice in lysis buffer (50 mM Tris-HCl, pH 7.4, 150 mM NaCl, 0.5% Triton X-100, protease inhibitor cocktail (0.2 mM PMSF, 50 mg/ml aprotinin, 1 mg/ml leupeptin, 1 mg/ml pepstatin) with occasional mixing for 30 min. Samples were centrifuged at 10 000 x g, 4°C for 15 min, and the supernatants containing the soluble fraction were transferred to clean tubes.

Immunoprecipitation

For the immunoprecipitation experiments, equal amounts of the cell lysate (200 mg of proteins) were incubated overnight at 4°C with 1 mg polyclonal anti-PARP-1 antibody (H-250, Santa Cruz Biotechnology). As a negative control, immunoprecipitation was performed with 50 ml anti-rabbit IgG (Santa Cruz Biotechnology). Samples were incubated for 1 h at room temperature under agitation, centrifuged at 10 000 x g. A/G-Agarose coupled beads with bound immunoprecipitated proteins were washed five times with lysis buffer and finally analyzed by SDS-PAGE in 12% gels. Immunoblot analysis was performed with anti-PARP-1 and anti-NF-κB antibodies.

RESULTS AND DISCUSSION

Post irradiation sequels in lymphocytes

Total body irradiation of experimental rats with low-LET ionizing radiation induced oxidative stress which was observed herein as increased activities of the major lymphocyte antioxidant enzymes total SOD (Fig. 1A), MnSOD (Fig. 1B), and catalase (Fig. 1A) 1 h after irradiation in blood plasma. Irradiation with sublethal (2.7 Gy, LD_{20}), mean lethal (5.4 Gy, LD50) and lethal (10.8 Gy) doses caused 1.6±0.1-, 1.3±0.08- and 1.1±0.06-fold increases in total SOD and 2.1±0.16-, 1.5±0.12- and 1.1±0.12-fold increases in CAT activities, respectively, compared to the respective control levels. Exposures to the mean lethal and in particular to the lethal dose was followed by smaller increases in both SOD and catalase activities. This was most likely because the high levels of ROS overwhelmed the cell's antioxidative capacity, producing extensive damage of different cellular components and major disruptions in cellular functioning, including antioxidant enzyme induction. In addition to the increase in antioxidant enzyme activities in the plasma after irradiation, exposure to sublethal, mean lethal and lethal doses induced a significant rise in MnSOD protein levels in lymphocytes in response to oxidative stress, as observed by Western analysis (1.76±0.15- and 1.8±0.15-fold, respectively; Fig. 1B).

To obtain an estimate of the extent of nuclear DNA damage, lymphocytes were isolated from peripheral blood 1 h after irradiation and subjected to the Comet assay (Fig. 2). The comets from control and irradiated lymphocytes were visually scored (Fig. 1A) and classified into categories (I-IV) describing increasing degrees of DNA damage (Fig. 1B). In untreated rats, 92% of the lymphocytes had undamaged DNA, observed as fluorescent spheres (category 0). After irradiation with sublethal and mean lethal doses, the DNA contained in about 70% of the lymphocytes exhibited different degrees of damage, observed as comets distributed in all four categories. After exposure to the lethal dose, 95% of the lymphocytes contained damaged DNA. Expressing DNA damage as values for the tail moment, considered to be a parameter that provides the most stable estimate for DNA damage (Lee et al., 2004), revealed that exposure to increasing doses of radiation produced comets with significantly higher tail moments (Fig. 2C). In control samples, the great majority of cells (90-95%) were without DNA tails, reflecting the absence of DNA breaks. The slightly lower value for the tail moment for comets obtained after exposure to the lethal dose as compared to

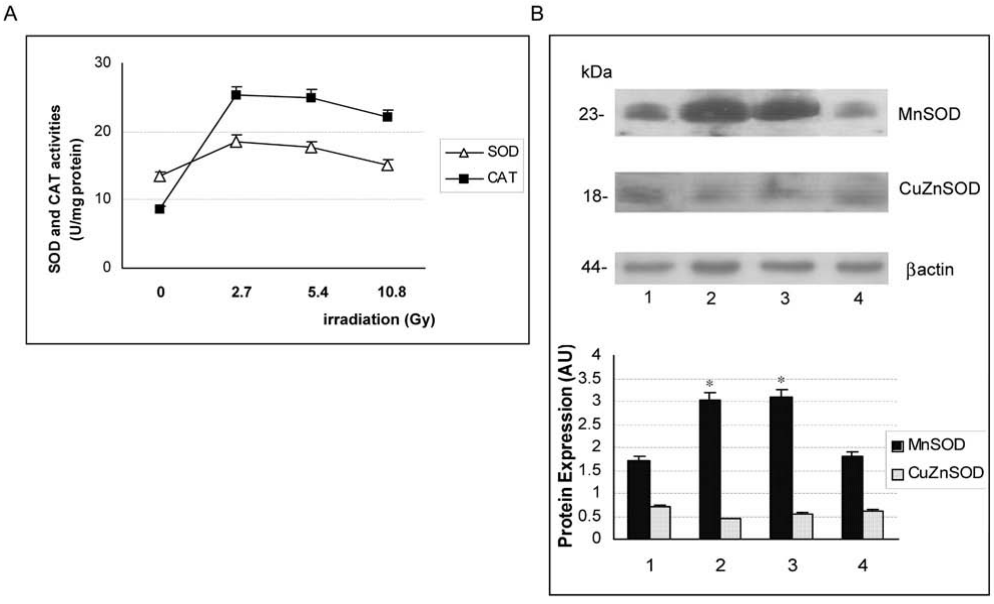

Fig. 1. Activities of plasma antioxidant enzymes after irradiation. A – total SOD (▪) and catalase (Δ) enzyme activities were measured in gels after non-denaturing PAGE, and are expressed as percent differences in densitometric units for each band. The results are representative of three independent experiments, expressed as means±SD, p<0,05. B – Western analysis of lymphocyte lysates 1 h after irradiation. The samples were probed with MnSOD (SOD2), CuZnSOD (SOD1) and b-actin antibody: lane 1 – control lymphocyte cell lysate; lanes 2, 3, 4 – lymphocyte cell lysates after whole body irradiation with 2.7, 5.4 and 10.8 Gy, and analysed by densitometry of individual bands and compared to the control. The results were obtained from 8 experimental rats and are expressed as means±SD (*p<0.05 significantly different from nonirradiated animals).

sublethal and mean lethal doses was probably due to DNA fragmentation to nucleosomal oligomer fragments as a result of accumulating double-strand incisions. The generated, relatively small pieces of DNA most likely readily disappeared during the comet assay, leaving behind empty "ghost"-cells with a smaller percentage of remaining DNA fluorescence (Collins, 2004). This assumption is supported by the following findings. The alkaline comet assay mainly detects single-strand breaks in DNA, but cannot distinguish between dead cells and cells with extensively damaged DNA but still capable of recovery (Henderson et al., 1998). Agarose gel electrophoresis of total nuclear DNA (Fig. 2) revealed the absence of oligonuclesomal DNA fragments in control samples (lane 1) and in rats irradiated with the sublethal dose (lane 2). Together with the results of the Comet assay, the latter finding indicates that DNA degradation after exposure to the sublethal dose was a result of single-stranded DNA breaks. The presence of oligonucleosomal fragments in mean lethal and lethal samples (lanes 3 and 4, respectively) points to the generation of a large number of double-strand DNA breaks after irradiation with higher doses.

The degree of activation of DNA damage repair after irradiation was assessed by examining the enzymatic activity of PARP-1, which assumes a central role in repair of ssDNA breaks. In response to DNA damage, PARP-1 is recruited to strand breaks that stimulate its catalytic activity and involvement in DNA repair. Total PARP-1 activity was examined in the lymphocyte lysate 1 h after irradiation (Fig. 3A). Exposure to 2.7 Gy elicited a 1.7±0.1-fold increase in PARP-1 activity (column 2) relative to its basal level of activity (column 1). Exposure to 5.4 and 10.8 Gy elicited lower (1.5±0.09- and 1.50±08-fold; columns 3 and 4, respectively) increases in activity. In extreme states of oxidative stress and ensuing DNA damage, PARP-1 overactivity causes cellular energy dysfunction that can culminate in a necrotic type of cell death (Virag et al. 1998). To preserve energy which

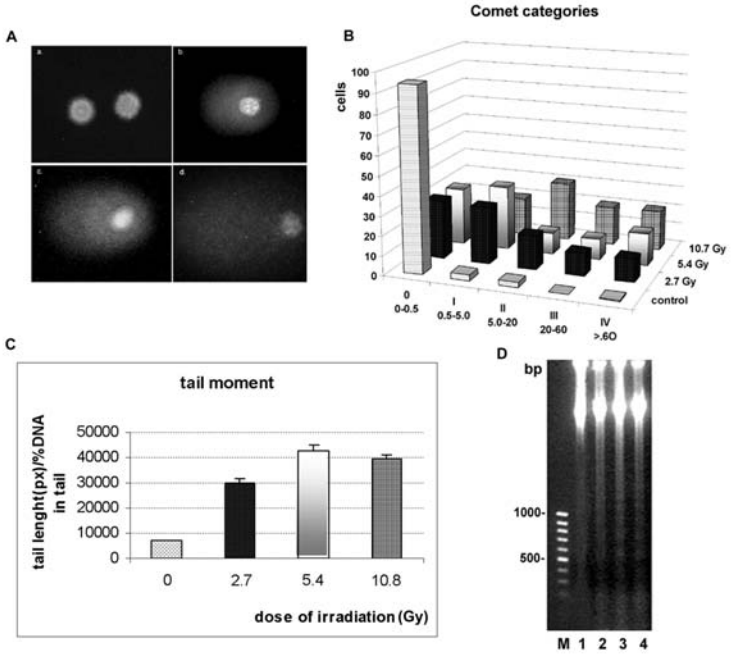

Fig. 2. Comet assay of lymphocytes after total body irradiation. A – Alkaline Comet assay images stained with Syber Green of control (a) and lymphocytes prepared 1 h after irradiation with 2.7 Gy (b), 5.4 Gy (c) and 10.8 Gy (d). B – distribution of comet categories after visual scoring. In class 0 comets observed in control lymphocytes, almost no DNA containing comet tail is visible; in class 4 comets most of the DNA is in the tail and the head is very small and hardly visible. C – quantification of lymphocyte DNA damage. The amount of DNA damage is presented as the tail moment (±S.E.M.), n=100, of control lymphocytes (lane 1) and lymphocytes isolated from rats irradiated with 2.7 Gy (lane 2), 5.4 Gy (lane 3) and 10.8 Gy (lane 4). Quantitative computer analysis of the fluorescence intensity of the migrated DNA was performed using TreTekCometScore™ Freeware (ver. 1.5). Approximately one hundred analyzed cells are depicted by each histogram. D – agarose gel electrophoresis of total lymphocyte DNA. Five μg of lymphocyte DNA isolated from control (lane 1) and rats irradiated with 2.7 Gy (lane 2), 5.4 Gy (lane 3) and 10.8 Gy (lane 4) 1 h after exposure was separated by 1.5% agarose gel electrophoresis. M – standard base pairs.

is required for the energy-sensitive steps during apoptosis, cells have developed a mechanism whereby PARP-1 activity and energy consumption are stopped by PARP-1 cleavage by cell death proteases. The generated specific PARP-1 cleavage fragments are recognized as markers for patterns of protease activity in unique cell death programs (Chaitanya et al., 2010). The cleavage of PARP-1 by several caspases, including caspase 3 which is activated in the intrinsic apoptotic pathway, results in the formation of an 89 kDa catalytic fragment that is released from the nucleus into the cytosol. The observed decline in PARP-1 catalytic activity (Fig. 3A) was the result of increasing PARP-1 cleavage detected after irradiation exposure. Quantification (Fig. 3C) of the lysate immunoblot profiles (Fig. 3B) showed decreasing amounts of full-length 113 kDa PARP-1 and increasing amounts of the 89 kDa PARP-1 apoptotic fragment with increasing irradiation dosage. Proteolytic processing by caspase 9 activates caspase 3 from its inactive procaspase form, resulting in downstream events involved in cell death, including this PARP-1 cleavage. Western analysis also revealed multi-fold increases in the amounts of 20 kDa active caspase 3 in lymphocyte lysates after exposure to increasing doses of irradiation (Fig. 3C). Together with the increasing presence of the PARP-1 apoptotic fragment, this result showed that exposure to higher doses of irradiation was followed by an increase in lymphocyte cell death by apoptosis. These findings also reveal that irradiation with the lethal dose generated DNA lesions above the capacity of the lymphocyte's DNA repair system, promoting extensive apoptotic cell death.

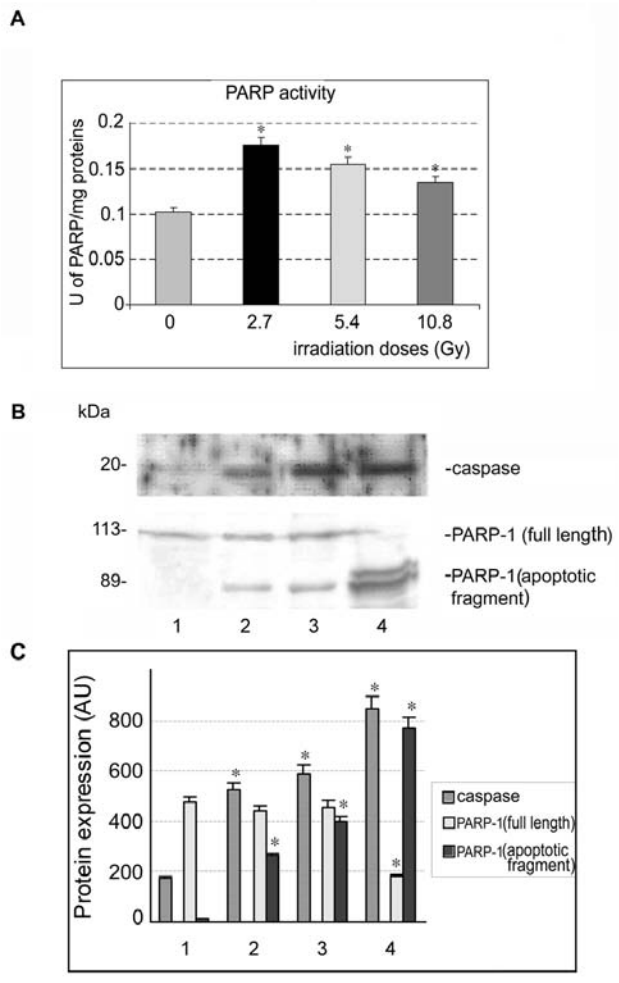

Fig. 3. PARP-1 and caspase-3 activities after exposure to total body ionizing irradiation. A – PARP-1 activity was measured with the Universal Colorimetric PARP-1 Assay Kit in lymphocyte lysates prepared from non-irradiated and rats 1 h after irradiation with 2.7 Gy, 5.4 Gy and 10.8 Gy. PARP-1 activity is expressed in units of activity per mg of proteins. B – Western analysis of lymphocyte lysates prepared from non-irradiated rats (lane 1) and 1 h after rats were irradiated with 2.7 Gy (lane 2), 5.4 Gy (lane 3) and 10.8 Gy (lane 4). The samples were probed with anti-caspase 3 and anti-PARP-1 antibodies. The anti-PARP-1 antibody bound to 116 kDa full length PARP-1 and its 89 kDa apoptotic fragment, as indicated. C – densitometric analysis of proteins after Western blotting (B). The numbers underneath three groups of columns denote the same treatments as described above. Results were obtained from three independent experiments and are expressed as means±SD, $p<0,05$.

Nuclear matrix-associated DNA repair centers

The major fraction of PARP-1, which plays a critical role in maintaining genome integrity through its involvement with DNA repair, resides on the nuclear matrix (Vidaković et al. 2004). To examine whether this sub-nuclear structure functions as a dynamic recruiting platform for components of DNA repair centers, the nuclear matrix was prepared from lymphocytes 1 h after whole-body exposure to increasing doses of radiation, and dynamic interactions of the nuclear matrix with two major protein participants in cell cycle arrest and DNA damage repair, p53 and PCNA, were investigated by Western analysis. Verification of the lymphocyte nuclear matrix was performed by immunoblot analysis with antibodies raised against the lamins, the major structural proteins of the nuclear matrix of most cells. The A/C lamins which characterize the liver cell (Fig. 4A, lane 1) and nuclear matrix structures from other tissues were absent in the lymphocyte nuclear matrices (Fig. 4A, lanes 2-4) where the major component is lamin B (Fig. 4A, lane 1), as was shown initially by Guilly et al. (1987). A radiation dose-dependent increase in the lamin B 45 kDa cleavage product produced by activated caspase 6 during the initial phase of apoptosis (Chang and Yang 2000; Ruchaud et al. 2002), was detected in the nuclear matrices (lanes 2-4).

Western analysis with anti-PARP-1 antibody (Fig. 4B) showed that total-body irradiation was accompanied by a radiation dose-dependent increase in partitioning of full-length PARP-1 with the nuclear matrix (1.6±0.14- and 2±0.14-fold relative to the control, after exposure to 2.7 and 5.4 Gy, respectively), as well as by a relative decline (1.7±0.14-fold) in PARP-1 association with the nuclear matrix after exposure to the lethal dose. These changes in PARP-1 association with the nuclear matrix were accompanied by a comparatively more gradual increase in association of the PARP-1 89 kDa apoptotic fragment with the nuclear matrix (Fig. 4B). The lower levels of the apoptotic PARP-1 fragments relative to full-length PARP-1 in the lymphocyte nuclear matrix as compared to the levels observed in the total lymphocyte lysate (Fig. 3B) suggest that proteolysis

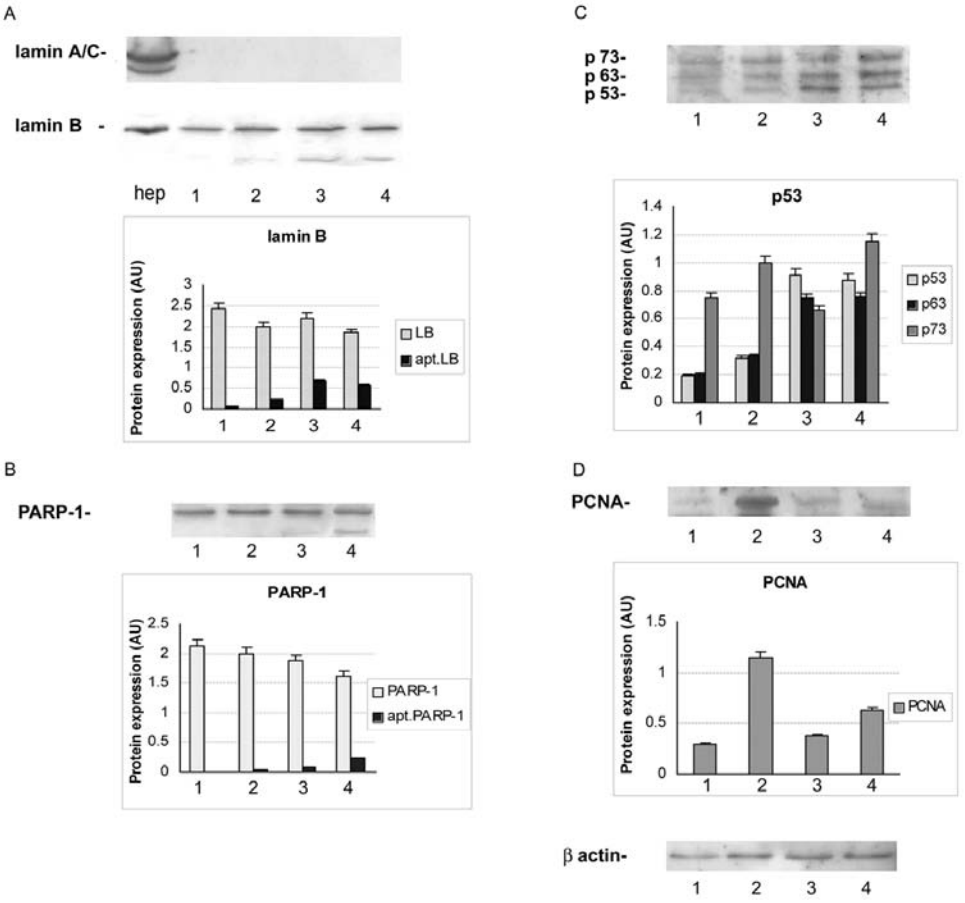

Fig. 4. Western analysis of lymphocyte nuclear matrix proteins after irradiation. A –hepatocyte (hep) and lymphocyte nuclear matrix proteins (lanes 1-4) probed with anti-lamin A/C and anti-lamin B (LB) antibodies. Control lymphocyte nuclear matrix (lane 1) and nuclear matrices isolated 1 h after total body irradiation with 2.7 Gy (lane 2), 5.4 Gy (lane 3) and 10.8 Gy (lane 4). The A/C lamins were not detected in lymphocyte nuclear matrices. The apoptotic lamin B fragment (apt LB) was observed in lanes 2-4). B – lymphocyte nuclear matrix proteins probed with anti-PARP-1 antibody (apt. PARP-1 – apoptotic PARP-1 fragment). The numbers denote the same treatments as above. C – lymphocyte nuclear matrix proteins probed with anti-p53 antibody. The numbers denote the same treatments as above. D – lymphocyte nuclear matrix proteins probed with anti-PCNA antibody. The numbers denote the same treatments as in Fig. 4A. β actin served as an internal standard.

of PARP-1 released it from the nuclear matrix in a more soluble form; this result is in agreement with Alvarez-Gonzalez et al. (1999) who showed that apoptosis promotes translocation of the 89 kDa PARP-1 fragment from nucleoli to the nucleoplasm.

PARP-1-interacting proteins may also be recruited to sites of DNA strand breaks to participate in the repair process. Vaziri et al. (1997) showed that PARP-1 activity and p53 accumulation are induced by DNA damage. Both proteins have subsequently been implicated as sensors of DNA damage (Wieler et al. 2003). Western-blot analysis with anti-p53 antibody (Fig 4C) revealed that exposure to increasing doses of ionizing radiation was accompanied by increased association of p53 with the nuclear matrix; the amounts of nuclear matrix-associated p53 after exposure to 2.7, 5.4 and 10.8 Gy increased 1.6±0.5-, 3.0±0.5- and 2.87±0.5-fold, respectively compared to the control value. The employed antibody also recognized two splicing variant-products of the TP53 gene, proteins p63 and p73. Significantly increased association of p63 with the nuclear matrix was observed after sublethal irradiation, and especially after

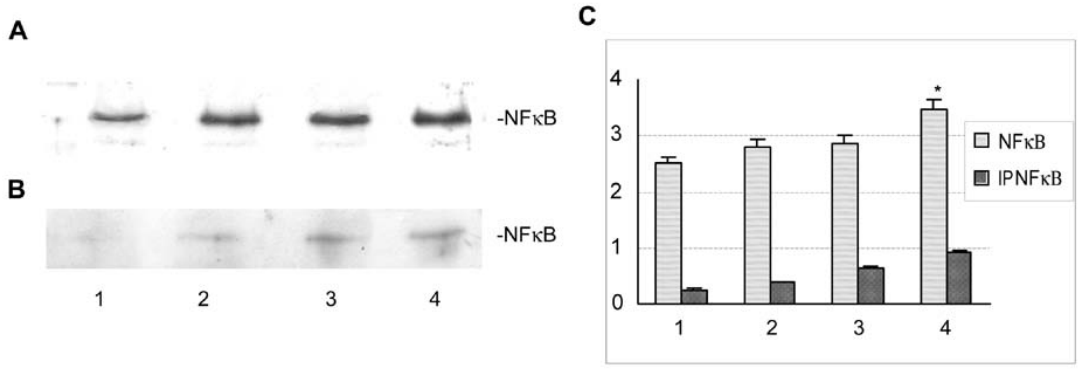

Fig. 5. NF-κB as a potential PARP-1 binding partner. A – Western analysis of lymphocyte nuclear matrix proteins with anti-NF-kB antibody. Nuclear matrices were isolated from non-irradiated lymphocytes (lane 1) and from lymphocytes prepared 1 h after irradiation with 2.7 Gy (lane 2), 5.4 Gy (lane 3) and 10.8 Gy (lane 4). B – immunoprecipitation assay performed with the lymphocyte cell lysate using anti-PARP-1 antibody. The immunoprecipitated samples from non-irradiated rats (lane 1) and samples from rats obtained 1 h after 2.7 Gy (lane 2), 5.4 Gy (lane 3) and 10.8 Gy (lane 4) were probed with anti-NF-kB antibody. C – quantification of the relative contents of NF-kB in the immunoprecipitated samples (IPNF-kB). The numbers denote the same treatments as above. Results were obtained from three independent experiments and are expressed as means±SD, $p<0.05$.

exposure to 5.4 and 10.8 Gy (4.4±0.9- and 4.1±0.9 fold, respectively). Protein p73 association with the nuclear matrix also increased but was comparatively less pronounced, with the highest increase of 1.6±0.2-fold detected after exposure to 10.8 Gy (Fig. 4C). Protein p63 is induced by DNA damage (De Laurenzi and Melino, 2000), whereas p53 and p73 exhibiting distinct mechanisms of induction (De Laurenzi et al., 2000).

Protein 73 is involved in the activation of p53-regulated genes involved in cell cycle arrest, growth suppression and apoptotic induction (Kaghad et al. 1997; Levrero et al. 2000), and the interplay between p73 and transcription factor NF-κB regulates the fate of lymphocytes (Cianfrocca et al. 2008). Protein p53 transcriptionally activates a number of genes in response to DNA damage, including PCNA, which functions as a sliding DNA clamp that localizes DNA polymerase δ to damaged DNA sites (Essers et al. 2005). Western analysis of the lymphocyte nuclear matrix with anti-PCNA antibody (Fig. 4D) revealed a 4.3±0.9 fold increase of lymphocyte nuclear matrix-associated PCNA (34 kDa) in rats after sublethal irradiation. After exposure to mean lethal and lethal irradiation, the association of PCNA with the nuclear matrix was similar (1.6±0.8- and 1.85±0.8-fold after 5.4 and 10.8 Gy, respectively). Previously we described a correlation between the nuclear matrix content of PCNA and cell proliferation, observed as a developmental-stage-specific decrease of PCNA association with the nuclear matrix in rat hepatocytes (Ivanović-Matić et al. 2000). Exposure to 2.7 Gy that elicited a peak in the cell's response to DNA damage coincided with maximal PCNA accumulation on the nuclear matrix. This result is in agreement with Karmakar et al. (2001) who concluded that X-ray-induced lesions in the DNA are largely repaired via the base excision repair (BER) pathway, with PCNA as one of the key components. During DNA damage repair, PARP-1 exchanges its binding partner lamin B for PCNA (Frouin et al. 2003; Vidaković et al., 2005). It is very likely that the decrease in PARP-1 activity detected after irradiation with a lethal dose (Fig. 3A) was initiated by its association with PCNA and finalized by the proteolytic degradation of PARP-1.

Integration of the decision-making process that determines cell fate on the nuclear matrix

High levels of free radicals that put cell survival at risk, act as messengers that directly or indirectly mediate the upregulation of the protein complex associated with NF-κB, which assumes a central role in

activating the cell's responses aimed at counteracting stress stimuli (Perkins, 2007). We next examined the association of transcription factor NF-κB with the lymphocyte nuclear matrix. Western analysis (Fig. 5A) revealed 1.6±0.09-, 1.7±0.09- and 2.0±0.09-fold increased associations of NF-κB p65 with the nuclear matrix after exposure to 2.7, 5.4 and 10.8 Gy ionizing radiation, respectively, compared to the control state. This result is consistent with the role of the nuclear matrix as a macromolecular platform that directs the activities of regulatory proteins through dynamic interactions (Ivanović-Matić et al., 2000; Bogojević et al., 2003). NF-κB regulates many physiological processes, including immune responses, inflammation, the cell's response to oxidative stress and cell death (Perkins, 2007). NF-κB inhibits apoptosis (Russo et al. 2001) by regulating the transcriptional activation of anti-apoptotic genes (Cianfrocca et al 2008), and PARP-1 has a critical role in NF-κB-dependent gene activation (Hassa and Hotinger, 1999). The fine balance between the cell's endogenous, opposing, destructive and prosurvival processes, attempts to maintain homeostasis and limit unnecessary damage after exposure to injurious stimuli. To obtain insight into the molecular relationship between NF-κB and PARP-1, we examined whether NF-κB and PARP-1 establish physicochemical connections in order to perform their functions in the course of lymphocytes' defense to the severely injurious signals induced by irradiation by immunoprecipitation experiments. Direct protein-protein interactions were observed between NF-κB (p65) and PARP-1 (Fig. 5B). Rats irradiated with 2.7, 5.4 and 10.8 Gy, exhibited 1.5±0.15-, 2.39±2.4- and 2.23±0.24-fold (Fig. 5B lanes 2, 3 and 4, respectively) increased protein-protein interaction of NF-κB with PARP-1, as compared to the control sample (Fig 5B). This findings is in agreement with Hassa et al. (2001) who described the direct interaction of PARP-1 and both subunits of NF-κB (p65 and p50), and the synergistic activation of NF-κB-dependent transcription by PARP-1.

CONCLUSION

The presented data reveal the involvement of the nuclear matrix in DNA repair and apoptosis through dynamic protein-protein interactions that coordinate the actions of the matrix-associated protein components: PARP-1, p53, PCNA and NF-κB. The ability of these molecules to establish functional interactions directly influences DNA repair and its outcome in apoptosis. Exposure to lower sublethal and mean lethal doses of irradiation promoted PARP-1 activation and recruited p53 and PCNA on the nuclear matrix. The lethal dose of irradiation caused extensive DNA damage and breakdown of the nuclear matrix-associated DNA repair centers, observed as caspase-mediated PARP-1 proteolysis and its decreased presence on the nuclear matrix and lamin B cleavage as the execution phase of the cell death program was initiated. Our results show that the crosstalk between the influx of injurious stimuli and the cell's defensive mechanisms is integrated in a process that resolves cell fate and is confined to the lymphocyte nuclear matrix.

Acknowledgments - This work was financed by the Ministry of Education, Science and Technological Development of the Republic of Serbia, Grant No. 173020.

Conflict of interest disclosure

The authors declare that there are no conflicts of interest.

REFERENCES

Alvarez-Gonzalez, R., Spring, H., Müller, M. and *A. Bürkle* (1999). Selective loss of Poly(ADP-ribose) and the 85-kDa fragment of Poly(ADP-ribose) polymerase in nucleoli during alkylation-induced apoptosis of HeLa cells. *J. Biol Chem.* **274,** 32122-32126.

Belgrader, P., Siegel, A.J. and *R.A. Berezney* (1991). Comprehensive study on the isolation and characterization of the HeLa S3 nuclear matrix. *J. Cell Sci*. **98,** 281-291.

Bogojević, D., Mihailović, M., Petrović, M., Dinić, S., Ivanović-Matić, S. and *G. Poznanović* (2003). Acute-phase-dependent binding affinity of C/EBPb from the nuclear extract and nuclear matrix towards the hormone response element of the a_2-macroglobulin gene in rat hepatocytes. *Gen. Physiol. Biophys*. **22,** 279-285.

Borehamd, R., Gale, K.L., Maves, S.R., Walker, J-A. and *D.P. Morrison* (1996). Radiation-induced apoptosis in human lym-

phocytes: Potential as a biological dosimeter. *Health Phys.* **71,** 685-691.

Chaitanya, G.V., Steven, A.J. and *P.P. Babu* (2010). PARP-1 cleavage fragments: signatures of cell-death proteases in neurodegeneration. *Cell Commun. Signal*, **8**, 31 (Open Access) http://www.biosignaling.com/content/8/1/31

Chang, H.Y. and *X. Yang* (2000). Proteases for cell suicide: functions and regulation of caspases. *Microbiol. Mol. Biol. Rev.* **6,** 821-846.

Chevion, S., Or, R. and *E.M. Berry* (1999). The antioxidant status of patients subjected to today body irradiation. *Mol. Biol. Int*. **47,** 1019-1027.

Cianfrocca., R., Muscolini, M., Marzano, V., Annibaldi A, Marinari B, Levrero M, Costanzo A and *L. Tuosto* (2008). RelA/NF-kB recruitment on the bax gene promoter antagonizes p73-dependent apoptosis in costimulated T cells. *Cell. Death Differ.,* **15,** 354-363

Collins, A.R. (2004). Comet assay for DNA damage and repair principles applications and limitations. *Mol. Biotechnol*. **26**, 249-61

De Laurenzi, V. and *G.Melino* (2000). Evolution of functions within the p53/p63/p73 family. *Ann. NY Acad. Sci*. **926**, 90-100.

Dendy, PP. and *M.J.P. Brugmans* (2003). Low dose radiation risks. *Brithish Journal of Radiology*, **76**, 674–7.

Dinić, S., Ivanović-Matić, S., Bogojević, D., Mihailović, M. and *G. Poznanović* (2000). C/EBPα and C/EBPβ are persistently associated with the rat liver nuclear matrix throughout development and the acute-phase response. *Cell Biol. Int.,* **24**, 691-698.

Essers, J., Theil, A.F., Baldeyron, C., van Cappellen, W.A., Houtsmuller, A.B., Kanaar, R. and *W. Vermeulen* (2005). Nuclear dynamics of PCNA in DNA replication and repair. *Mol. Cell Biol*. **25**, 9350-9359.

Fackelmayer, F.O. (2004). Nuclear Architecture and gene expression in the quest for novel therapeutics. *Curr. Pharm. Design* **10**, 1-10.

Farber, J.L. (1994). Mechanisms of cell injury by activated oxygen species. *Environ. Health Perspect.* **102**, 17-24.

Feinendegen, L.E. (2003). Relative implications of protective responses versus damage induction at low-dose and low-dose rate exposures, using the microdose approach. *Radiat. Prot. Dosim*. **104**, 337–46.

Feinendegen, L.E. (2005). Evidence for beneficial low level radiation effects and radiation hormesis. *Brit. J Radiol*, **7,** 83–7.

Frouin, I., Maga, G., Denegri, M., Riva, F., Savio, M., Spadari, S., Prosperi, E. and *A.I. Scovassi* (2003) Human proliferating cell nuclear antigen, poly(ADP-ribose) polymerase-1 and p21. *J Biol. Chem.* **278**, 39265-39268.

Grdović, N. and *G. Poznanović* (2003). Characterization of an Mg^{2+}-dependent endonucleolytic activity of the rat hepatocyte nuclear matrix. *Comp. Biochem. Physiol. Part B.* **136,** 495-504.

Grdović, N., Vidaković, M. and *G. Poznanović* (2005). Binding of a 23 kD endonuclease to the rat liver nuclear matrix. *Gen. Physiol. Biophys.* **24,** 99-111.

Guilly, M.N., Bensussan, A., Bourge, J.F., Bornens, M. and *J.C. Courvalin* (1987). A human T lymphoblaste cell line lacks lamins A and C. EMBO J **6,** 3795-3799.

Hassa, P.O., Čović, M., Hasan, S., Imhof, R. and *M.O. Hottiger,* (2001). The enzymatic and DNA binding activity of PARP-1 are not required for NF-kappa β coactivator function. *J Bio. Chem.* **276**, 45588-97.

Hassa, P.O. and *O. Hottinger* (1999). A role of poly (ADP-ribose) polymerase in NF- kappa β transcriptional activation. *Biol. Chem.*, **380,** 953-959.

Henderson, L., Wolfreys, A., Fedyu, J. and *S. Windebank* (1998). The ability of the Comet assay to discrminate between genotoxins and cytotoxins. *Mutagenesis,* **13**, 89-94

Holt, S.M., Scemama, J-L., Panayiotidis, M.I. and *A.G. Georgakilas* (2009). Compromised repair of clustered DNA damage in the human acute lymphoblastic leukemia MSH2-deficient NALM-6 cells. *Mutat. Res-Gen Tox. En,* **674**, 123-130.

Ivanović-Matić, S., Dinić, S., Vujošević, M. and *G. Poznanović* (2000). The protein composition of the hepatocyte nuclear matrix is differentiation-stage specific. *IUBMB Life* **49**, 511-517.

Kaghad, M., Bonnet, H., Yang, A., Creancier, L., Biscan, J., Valent, A., Minty, A., Chalon, P., Lelias, J. and *M. Dumont* (1997). *Cell* 90:809–819.

Karmakar, P., Balajee, A.S., and *A.T. Natarajan* (2001). Analysis of repair and PCNA complex formation induced by ionizing radiation in human fibroblast cell lines. *Mutagenesis*, **16,**225-232.

Klauning, J.E., Xu, Y., Isenberg, J.S., Bachowsk, S., Kolag, K.L., Jiang, J., Stevenson, D.E. and *E.F. Walborg Jr.* (1998). The role of oxidative stress in chemical carcinogenesis. *Environ. Health Perspect.* **106**, 289-295.

Laemmli, U.K. (1970). Cleavage of structural proteins during the assembly of heat of bacteriophage T4. *Nature*, **227**, 680-685.

Lee, E., Oh, E, Lee J, Sul, D. and *J. Lee* (2004). Use of the tail moment of the lymphocytes to evaluate dna damage in human biomonitoring studies. *Toxicol. Sci.,* **81**, 121-132.

Levrero, M., De Laurenzi, V., Costanzo, A., Sabatini, S., Gong, J., Wang, Y.J. and *G. Melino* (2000). The p53/p63/p73 family of transcription factors: overlapping and distinct functions. *Journal Cell Sci.,* **113**, 1661-1670.

Linnemann, A.K., Platts, A.E. and *S.A. Krawetz* (2009). Differential nuclear scaffold/matrix attachment marks expressed genes. *Human Mol. Genetics,* **18**, 645-654.

Loft, S. and *H.E. Poulsen* (1996). Cancer rise and oxidative DNA damage in man. *J Mol. Med.*, **74**, 297-312.

Lowry, O. H., Rosebrough, W. J., Farr, A. L. and *R. J. Randall* (1951). Protein measurements with the Folin phenol reagent. *J Biol. Chem.,* **193**, 429-432.

Mori, M. and *C. Desaintes* (2004). Gene expression in response to ionizing radiation: An overview of molecular features in hematopoietic cells. *J. Biol. Reg. Homeost. Agents,* **18,** 363-371.

Oberly, L. W. and *T. D. Oberly* (1986). Free radicals, cancer and aging. *Free Radical Aging Degenerative Dis.* pp. 325-371, Alan R liss Inc, New York.

Oberley, L.W. and *D.R. Spitz* (1984). Assay of superoxide dismutase activity in tumor tissue. *Methods Enzymol.* **105**, 457-469.

Olive, P.L., Banath, J.P. and *R.E. Durand* (1990a). Heterogeneity in radiation-induced DNA damage and repair in tumor and normal cells measured using the "comet" assay. *Radiat. Res.* **122**, 86-94.

Perkins, N.D. (2007). Integrating cell-signalling pathways with NF-κB and IKK function *Nat. Rev. Mol. Cell Biol.* **8**, 49-62.

Poznanović, G., Grujić, V., Ivanović-Matić, S. and *Lj. Ševaljević* (1994). Regions of the haptoglobin 5' flanking gene sequence show different binding affinities to nuclear matrix proteins during the acute phase response. *J. Biochem*., **115**, 422-428.

Poznanović, G., Grujić, V., Ivanović-Matić, S. and *S. Šekularac* (1996). Posttranslational modifications of the haptoglobin gene 5' flanking DNA-binding nuclear matrix proteins during the acute phase response. *Cell Biol. Int*., **20,** 751-762.

Poznanović, G., Vidaković, M., Ivanović-Matić, S. and *V. Grujić* (1999). Identification of nuclear matrix and associated proteins that bind the haptoglobin gene *cis*-element. *IUBMB Life,* **48**,1-6.

Ruchaud, S., Korfali, N., Villa, P., Kottka, T.J., Dingwall, C., Kaufmann, S.H. and *W. Earnshaw* (2002). Caspase 6 gene disruption reveals a requirement for lamin A cleavage in apoptotic chromatin condensation. *EMBO J*, **21,** 1967-77.

Russo S.M., Tepper, J.E., Baldwin, A.S.Jr, Liu, R., Adams, J., Elliott, P. and *J.C.Cusack Jr.* (2001). Enhancement of radiosensitivity by proteasome inhibition: implications for a role of NF-kappaB**.** *Int. J Radiat. Oncol. Biol. Phys***. 50(1),** 183-93.

Singh, N.P., Stephens, R.E. and *E.L. Schneider* (1994). Modification of alkaline microgene electrophoresis for sensitive detection of DNA damage. *Int. J. Radiat. Biol.* **66,** 23-28.

Sun, Y., Elwell, J.H. and *L.W. Oberley* (1988). A simultaneous visualization of the antioxidant enzymes glutathione peroxidase and catalase on polyacrylamide gels. *Free Radic. Res. Commun*. **5**, 67-75.

Towbin, H., Staehelin, T. and *J. Gordon* (1979). Electrophoretic transfer of proteins from polyacrilamide gels to nitrocellulose sheets: procedure and some aplications. *Proc. Natl. Acad. Sci. USA*, **76**, 4350-4354.

Vaziri, H., West, M.D., Allsopp, R.C. et al. (1997). ATM-dependent telomere loss in aging human diploid fibroblasts and DNA damage lead to the posttranslational activation of p53 protein involving poly(ADP-ribose)polymerase. *EMBO*, **16,** 6018-6033.

Veuger, S. J., Hunter, J. E. and *B. W. Durkacz* (2009). Ionizing radiation-induced NF-kB activation requires PARP-1 function to confer radio-resistance. *Oncogene,* **28,** 282-842.

Vidaković, M., Grdović, N., Quesada, P., Bode, J. and *G. Poznanović* (2004). Poly(ADP-ribose) polymerase-1: Association with nuclear lamins in rodent liver cells. *J. Cell Biochem*. **93,** 1155-1168.

Vidaković, M., Poznanović, G. and *J. Bode* (2005). DNA break repair: Refined rules of an already complicated game. *Biochem. Cell Biol/Biochim. Biol. Cell*, **83,** 365-373.

Virag, L., Scott, G.S., Cuzzocrea, S., Marmer, D., Salzman, A.L. and *C. Szabo* (1998). Peroxynitrite induced thymocyte apoptosis: the role of caspases and poly(ADP-ribose) synthetase (PARS) activation. *Immunology,* **94**, 345-355.

Wieler, S., Gagne, J-P., Vaziri, H., Poirier, G.G. and *S. Benchimol* (2003). Poly(ADP-ribose) polymerase-1 is a positive regulator of the p53-mediated G1 arrest response following ionizing radiation. *J. Biol. Chem.,* **278**, 18914-18921.